Copyright © 2004 Tech Science Press CMES, vol.5, no.3, pp.279-286, 2004

# Frequency-Shifting Analysis of Electrostatically Tunable Micro-Mechanical Actuator

**Wan-Sul Lee, Kie-Chan Kwon, Bong-Kyu Kim, Ji-Hyon Cho, and Sung-Kie Youn** [1]

**Abstract:** A numerical approach for eigenvalue analysis of the electrostatically tunable micro-mechanical actuators is presented. An efficient algorithm for calculating the natural frequency shifting in the micro-mechanical actuators due to applied DC turning voltage is proposed. In the calculations of the coupled field problem, the three-dimensional FEM/BEM approaches and iterative staggered algorithm are employed. The numerical examples for actually fabricated actuators are presented and the numerical analysis results are compared with experimental data.

**keyword:** micro-mechanical actuator, electrostatic field, natural frequency shifting, coupled field analysis.

## 1 Introduction

The micro-mechanical resonators, which are driven by electrostatic force, are widely used in active micro-electromechanical systems because of high reliability and low power consumption. Electrostatic micro-actuators are usually operated at their resonant frequencies, which will give the maximum displacement amplitude and the highest operating efficiency [Tang, Nguyen and Howe (1989); Tang, Lim and Howe (1992)]. The resonant frequency tuning of the electrostatic micro-actuator is required for post-fabrication adjustment of resolution and bandwidth in order to remove the effect of fabrication error. The resonant frequency of a micro-actuator can be generally tuned by applying DC bias voltage.

Previous works on the numerical analysis of tunable electrostatic actuators used very simplified models in which micro-mechanical actuators are assumed as single mass-spring systems [Adams et. al. (1995); Seo, Cho and Youn (1998); Francais (2000)]. However, actuator systems must be modeled to continuum structures [Ljung, Bachtold and Spasojevic (2000)] because the actuators assumed as rigid body in previous works are generally deformable. Moreover, in real actuator situations, the electrostatic field and the elastic deformation field of the system are 3-dimensionally coupled. Some advanced numerical approaches, which can treat continuous fields, is used only in the calculation of the electrostatic force applied on the device [Lee and Cho (1998); Ye and Mukherjee (2000)]. In order to accurately predict the behavior of the real system, the analysis of the coupled fields in 3-D continuous system and an algorithm for evaluating the influences of electrostatic field on natural frequency are necessary.

In this work, a numerical scheme for eigenvalue analysis of electrostatically tunable micro-mechanical actuators is proposed. The finite element method and the boundary element method [Katsikadelis and Nerantzaki (2000), Gaul, Fischer and Nackenhorst (2003), Han and Atluri(2003)] are very useful methods to analyze such micro-mechanical continuum systems. We use the boundary element method (BEM) and the finite element method (FEM) for the 3-D analysis of electrostatic field and deformation of devices respectively. And also an iterative staggered algorithm is used for coupled analysis of two fields. In order to consider the effects of electrostatic field on natural frequency, an equivalent stiffness matrix for electrostatic tuning voltage is introduced. We can perturb the equilibrium structure using a concerned eigenvector of operating mode and then linearize the corresponding electrostatic force variation in order to determine the equivalent stiffness. For examples, a simple beam-shaped structure, a tunable electrostatic micro-mirror and a repulsive micro comb-structure are analyzed and the numerical analysis results of frequency shifting are compared with the experimental data.

[1] Department of Mechanical Engineering, KAIST, 373-1, Guseong-dong, Yuseong-gu, Daejon, 305-701, KOREA

## 2 Numerical Procedures

### 2.1 Coupled Field Analysis

Electrostatically driven micro-actuator system is governed by the electrostatic driving force and the elastic restoring force. Since the structure deforms due to the applying electrostatic forces and then the electrostatic fields are modified by corresponding structural deformation, this actuator is an electrostatic-elastic coupled system. A coupled analysis of the electrostatic and elastic deformation fields needs to achieve the equilibrium state. An iterative staggered algorithm is employed in order to perform the electrostatic-elastic coupled analysis [Shi, Ramesh and Mukherjee (1996)]. A simple flow chart of the staggered algorithm for the electrostatic-elastic coupled field analysis is shown in Fig. 1.

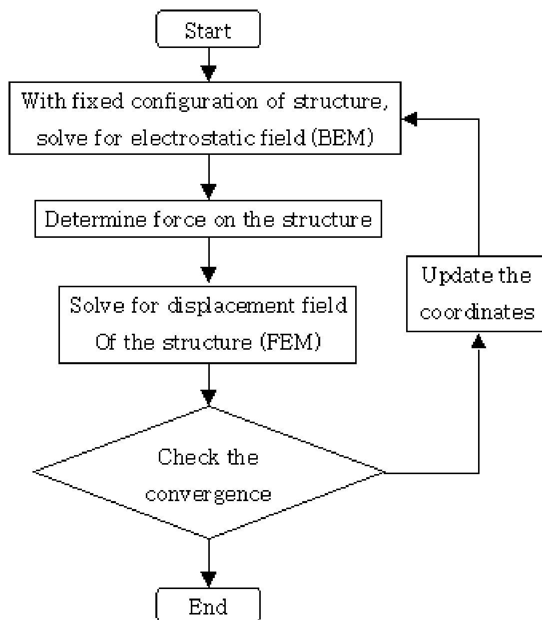


**Figure 1** : Flow chart of the electrostatic-elastic coupled field analysis

The electrostatic field induced by the electric potential applied on the electrodes is analyzed by BEM. When conductors are surrounded with homogeneous dielectric medium, the electric potential of each conductor is constant. The charge density on the conductor surface can be calculated as follow:

$$q(\boldsymbol{x}) = -\varepsilon \frac{\partial \phi(\boldsymbol{x})}{\partial x_i} n_i(\boldsymbol{x}) \tag{1}$$

where $q(\boldsymbol{x})$ is the charge density at a point $\boldsymbol{x}$ on the conductor surface, $\phi(\boldsymbol{x})$ the electric potential of conductor, $\varepsilon$ the dielectric permittivity of media and $\boldsymbol{n}(\boldsymbol{x})$ the normal vector to the inside of conductor. And then the electrostatic forces on the conductor surface can be obtained as follow:

$$\boldsymbol{f}(\boldsymbol{x}) = -\frac{1}{2}\frac{q(\boldsymbol{x})^2}{\varepsilon}\boldsymbol{n}(\boldsymbol{x}) \tag{2}$$

The deformation of the structure caused by electrostatic force is calculated with FEM. Then the electrostatic field is modified due to the structural deformation and then the electrostatic forces are updated again. The iterative process continues until the equilibrium is achieved.

### 2.2 Frequency Shifting Analysis

When the dynamic deformation of a structure is considered, the equation of motion can be written as follows.

$$\boldsymbol{M}\ddot{\boldsymbol{U}} + \boldsymbol{K}\boldsymbol{U} = \boldsymbol{F} \tag{3}$$

where $\boldsymbol{K}$, $\boldsymbol{M}$, and $\boldsymbol{F}$ are, respectively, the stiffness matrix, the mass matrix, and the load vector of the system and made by finite element approximation of the structure. Above equation of motion can be uncoupled to single degree-of-freedom equations by the linear coordinate transformation defined by eigenvectors [Meirovitch, (1980)]. Each uncoupled equation is related to only one eigenmode and can be regarded as single-degree-of-freedom system. Thus after uncoupling of the motion, we can easily separate the effects of the electrostatic field on each mode.

Let us consider one resonant frequency of the structure. Only one single-degree-of freedom governing equation can be obtained instead of whole system of motion. The equation of motion can be expressed as follow:

$$m\ddot{q} + kq = f \tag{4}$$

where $q$ denotes the generalized coordinate for a concerned eigenmode, $k$ is the lumped stiffness, $m$ is the lumped mass, and $f$ is the lumped force. Each lumped parameter is defined as follow:

$$m = \boldsymbol{Q}^T\boldsymbol{M}\boldsymbol{Q} \tag{5}$$

$$k = \boldsymbol{Q}^T\boldsymbol{K}\boldsymbol{Q} \tag{6}$$

$$f = \boldsymbol{Q}^T \boldsymbol{F} \tag{7}$$

where $\boldsymbol{Q}$ is the concerned eigenvector. Simply the eigenvalue of equation (4) is $k/m$. For an example, Fig. 2 shows a simple beam structure and its concerned eigenmode shape.

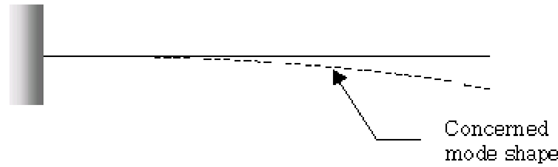


**Figure 2** : A simple beam structure and its mode shape

The generalized coordinate and the applied force can be decomposed into a static equilibrium part and a deviation part from the static equilibrium. The equation of motion can be written as follows:

$$m\Delta\ddot{q} + k(q_0 + \Delta q) = f_0 + \Delta f \tag{8}$$

where $q_0$ and $f_0$ are, respectively, the generalized coordinate value and the static force at the equilibrium. And then $\Delta q$ is the perturbed increment of the generalized coordinate from the equilibrium, and $\Delta f$ is the corresponding deviation of static force.

Because the electrostatic force balances with the restoring force by elastic deformation at the static equilibrium, the equation of motion can be described in terms of incremental variables.

$$m\Delta\ddot{q} + k\Delta q = \Delta f \tag{9}$$

The total force increment in above equation can be explained as a sum of the external force increment, $\Delta f_{ext}$, and the electrostatic tuning force increment, $\Delta f_{tuning}$. The electrostatic tuning force increment comes from the deviation of the electrostatic field due to $\Delta q$. $\Delta f_{tuning}$ can be approximated by first derivative of electrostatic force, for a small $\Delta q$.

$$\Delta f = \Delta f_{ext} + \Delta f_{tuning} = \Delta f_{ext} + \frac{\partial f_e}{\partial q}\Delta q \tag{10}$$

where $f_e$ is the electrostatic force applied to the structure for static equilibrium. From equation (9) and (10), the equation of motion can be modified as follow:

$$m\Delta\ddot{q} + \left(k - \frac{\partial f_e}{\partial q}\right)\Delta q = \Delta f_{ext} \tag{11}$$

The lumped stiffness of the system is modified as much as $(-\partial f_e/\partial q)$. Thus the modified eigenvalue can be expressed as follow:

$$\lambda = \frac{k - \frac{\partial f_e}{\partial q}}{m} = \frac{k - k_{tun}}{m} \tag{12}$$

The electrostatic tuning stiffness, $k_{tun}$, can be calculated by finite difference method. At first, system configuration is modified by $\Delta U = \Delta q Q$. Fig. 3 shows the equilibrium states and a small perturbation of the system. Then the variation of electrostatic forces is evaluated at the perturbed configuration. Finally, the approximate tuning stiffness is calculated as follow:

$$k_{tun} = \frac{\Delta f_e}{\Delta q} = \frac{\boldsymbol{Q}^T \Delta \boldsymbol{F}_e}{\Delta q} \tag{13}$$

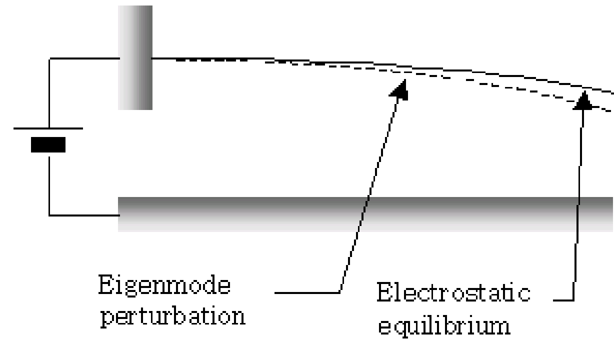


**Figure 3** : Equilibrium state and perturbation

where $\Delta F_e$ is electrostatic force increment vector. Using equation (12) and equation (13), the eigenvalue tuned by electrostatic field, can be obtained.

$$\lambda = \frac{k - k_{tun}}{m} = \left(k - \frac{\boldsymbol{Q}^T \Delta \boldsymbol{F}_e}{\Delta q}\right)/m \tag{14}$$

## 3 Numerical Examples

### *3.1 Beam type Resonator*

The natural frequency shifting of a simple beam-type structure is computed to present the reasonability of the

proposed numerical approach. This resonator structure is composed of two conductors, a doubly clamped beam and a substrate, and its schematic diagram is shown in Fig. 4. The beam is assumed as Silicon and its density and elastic modulus are, respectively, 2330 $kg/m^3$ and 130 GPa.

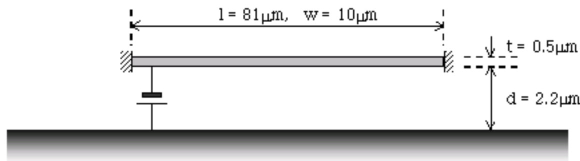


**Figure 4** : Structure of beam type resonator

The beam is deformed by the electrostatic force, which is induced by the voltage difference between the electrodes. The original natural frequency of the beam is 620kHz and then the natural frequency can be tuned by changing the intensity of electrostatic field as explained in the previous sections. In the present approach, the boundary element method is used for the analysis of electrostatic field between two electrodes and the finite element method is used for the structural analysis of beam. From the results of coupled field analysis and perturbation analysis, the tuned natural frequency can be calculated using equation (14).

Fig. 5 shows the first mode shape of the structure, which is calculated by the finite element method, and this mode may be primarily concerned with actuator operation. The configuration at the equilibrium state is superposed by the scaled eigenmode profile whose maximum displacement is 0.1% of the maximum displacement at equilibrium to calculate the increment of the external electrostatic force.

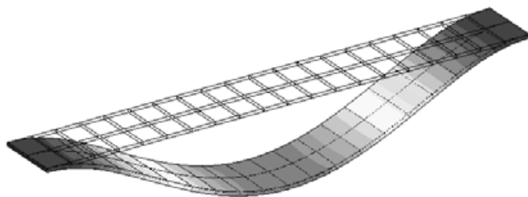

**Figure 5** : Concerned mode shape of the beam structure

Applying the DC bias voltage of 10V, the charge density distribution on the conductor surface at the equilibrium state, can be calculated by the boundary element method and are shown in Fig. 6. From this distribution, the electrostatic force can be obtained by equation (2). Fig. 7 shows the distribution of the electrostatic force on the beam at the equilibrium state. The increment of electrostatic force, the effective stiffness and then the shifted natural frequency is calculated with the eigenmode perturbation on the equilibrium configuration. Fig. 8 shows the tuned frequency for the tuning voltages. It is observed that the natural frequency decreases with the increase of DC bias voltage and the original frequency of 620kHz is shifted down to the 546kHz for the DC bias voltage of 60V. It is noted that the proposed approach can effectively analyze the frequency shifting by electrostatic field change.

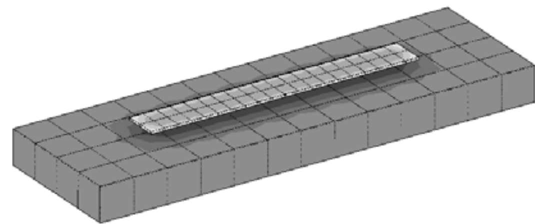

**Figure 6** : Charge density distribution on the conductor surface at equilibrium (10V)

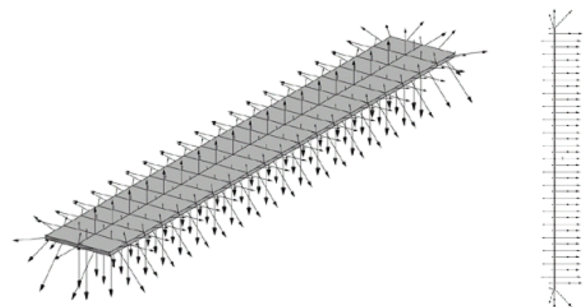

**Figure 7** : Electrostatic force at equilibrium (10V)

### 3.2 *Tunable Micromirror System*

The electrostatic tunable micromirror is applicable to a wide variety of static and dynamic opto-mechanical micro devices, including optical micro-switches, optical

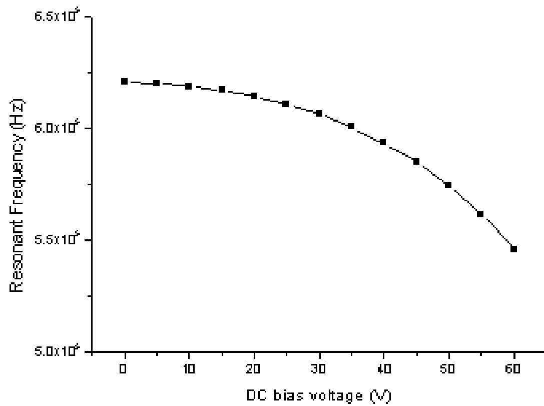


**Figure 8** : Computed resonant frequency of the beam structure for tuning voltages

shutters, laser beam choppers, optical filters and optical couplers. In order to verify the validity of proposed method, we analyze the frequency shifting of a micromirror actually devised, fabricated, and tested. In Fig. 9, a SEM photograph of the micromirror fabricated by an anisotropic etching of (110) silicon wafer is presented [Seo, Cho and Youn (1998)]. Two pairs of boron-diffused micro-beams suspend a bulk-micro machined electrostatic micromirror. Fig. 10 shows the schematic diagram of structure with a counter electrode. The density and the elastic modulus of Silicon are, respectively, 2330 $kg/m^3$ and 130 GPa.

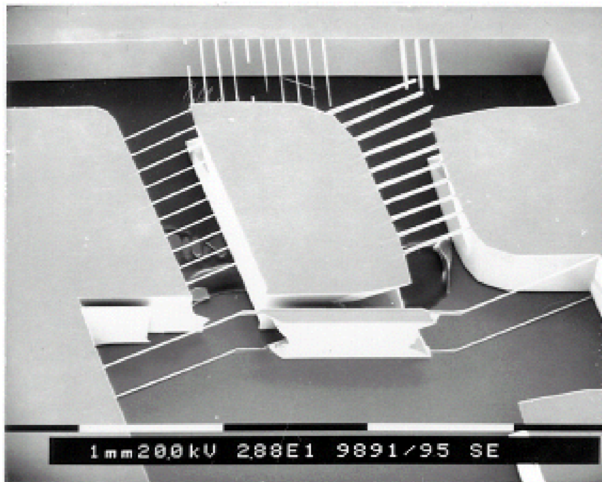


**Figure 9** : SEM Photograph of micromirror structure

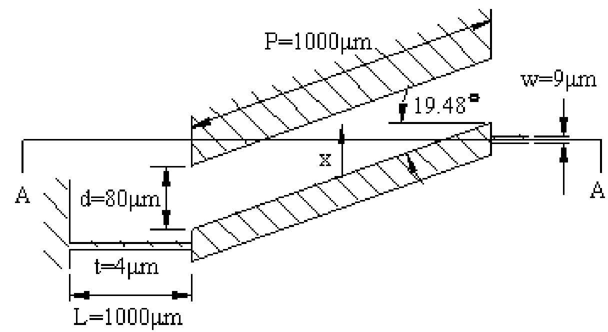


**Figure 10** : Top view of the silicon micromirror with a counter electrode

The vertical micromirror can be driven parallel to the silicon substrate by the electrostatic actuating force. The electric potential difference between two electrodes generates the electrostatic field and then the corresponding electrostatic forces are applied on the vertical micromirror surface. The net force on the micromirror may be attractive in the x-direction, i.e. parallel to the substrate. The frequency tuning must be accomplished within the allowable range because, at a large voltage over the allowable limit, the movable part will become unstable and be stuck to the fixed conductor. In a static performance test, stable operation of micromirror has been observed up to the threshold voltage of 330V.

The movable part is actuated by applying the driving AC voltage at usually natural frequency and that natural frequency of the micromirror can be tuned by changing the DC bias voltage. In the experiment, the resonant frequency of the fabricated micromirror can be found as the frequency at which the amplitude of displacement has the maximum value for various actuating frequencies. In numerical analysis, the tuned natural frequency can be calculated by equation (14). Fig. 11 shows the concerned mode shape of the micromirror, calculated by finite element analysis. In this case, since the first mode of the vertical direction is not concerned with the operating mode of actuator, the second mode of the horizontal direction must be considered. The resonant frequency tuning is analyzed by perturbing with this concerned mode shape profile. The 0.1% perturbation of the maximum displacement is used in the calculation.

Fig. 12 and Fig. 13, respectively, show the charge density and electrostatic force on the micromirror surface when the system is in the equilibrium for the tuning voltage

**Figure 11** : Concerned mode shape of the micromirror

of 150V. From the distribution of electrostatic force, we can see that the operation mode of mirror is in the horizontal direction. Fig. 14 compares the computed and measured frequency of the frequency tunable micromirror for the tuning voltages. From Fig. 14, 23% reduction of the resonant frequency is measured by test, and 25.3% reduction of resonant frequency is calculated for the tuning voltage increase of 300V. Considering the fact that the geometrical irregularities in the fabricated structure are not exactly reflected in the computational model, the differences seem to be moderated. It is noted that the numerical results are very close to the experimental results and the proposed numerical scheme is reasonable.

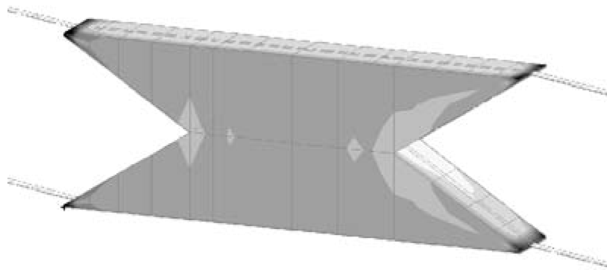

**Figure 12** : Charge density on mirror surface at equilibrium (150V)

### 3.3 *Repulsive Micro Comb-Structure*

As another example, the repulsive micro comb-structure [Lee and Cho (1998)] as shown in Fig. 15(a) and Fig. 15(b) have been analyzed. In this micro-system, there are 32 sets of comb-teeth and each set has three types of electrode, two negative electrodes (electrode I and II) and a positive electrode (electrode III). This micro actuator uses the repulsive force between two electrodes that have

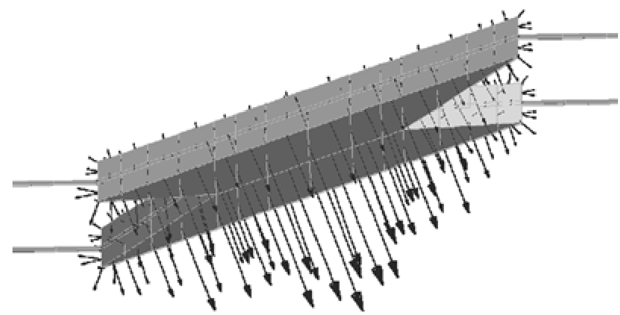

**Figure 13** : Electrostatic force on mirror surface at equilibrium (150V)

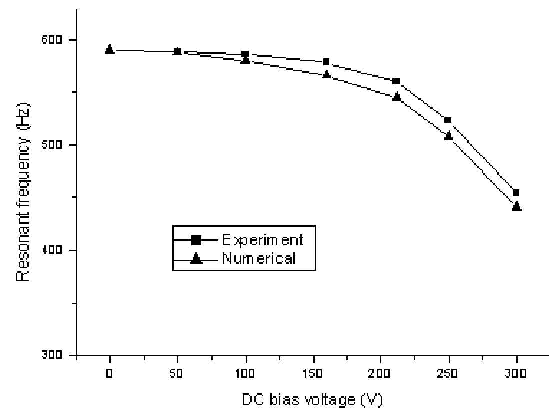


**Figure 14** : Computed and measured resonant frequency of the micromirror for tuning voltages

the same negative electric potentials. The movable part can be driven parallel to the silicon substrate by the repulsive electrostatic force. In this case, there is no sticking between electrodes by large tuning voltage. However frequency tuning will be saturated by force equilibrium due to two surrounding electrodes (electrode II).

The first vibration mode of this system has the mode shape of vertical direction that is independent of the actuator driving mode. The second mode of the horizontal direction must be considered. The resonant frequency tuning is analyzed by perturbing with the concerned mode shape profile. The 0.1% perturbation of the maximum displacement is used in the calculation.

Fig. 16 and Fig. 17, respectively, show the electrostatic

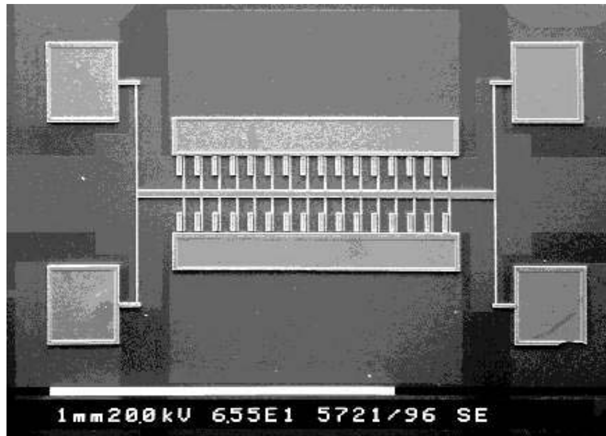


(a) The whole structure

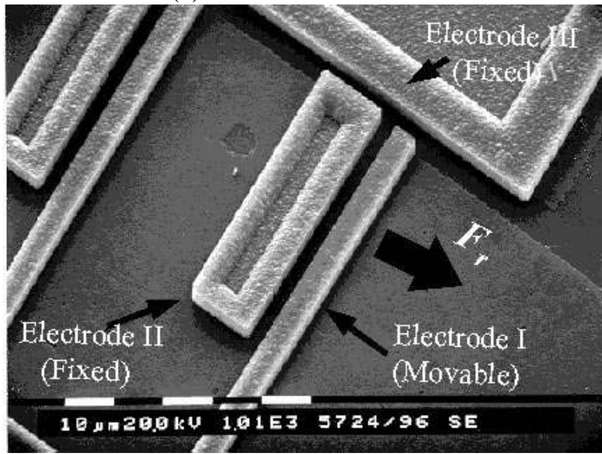


(b) Three types of electrodes

**Figure 15** : SEM photographs of the micro com-structure

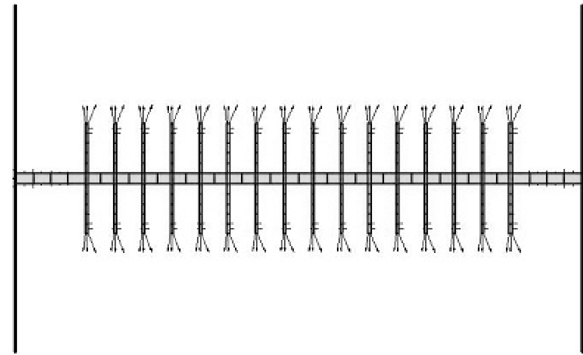

**Figure 16** : Electrostatic force on the structure surface at equilibrium (100V)

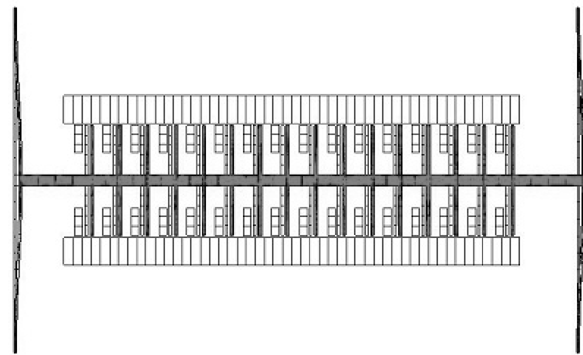

**Figure 17** : System configuration at equilibrium (100V)

force on the movable micro comb-structure surface and the corresponding system configuration when the system is in the equilibrium for the tuning voltage of 100V.

Fig. 18 compares the computed and measured frequency of the frequency tunable micromirror for the tuning voltages. From Fig. 18, there is 13% error of the resonant frequency between the experiment and the numerical analysis at 80 Volt and there are very small errors in other cases. It is noted that the numerical results are very close to the experimental results and the proposed numerical scheme is reasonable.

## 4 Conclusions

A numerical approach for natural frequency (eigenvalue) shifting analysis of electrostatically tunable micro-mechanical actuators is presented. The electrostatic micro-actuators are modeled as 3-dimensional continuum structures and then the electrostatic forces and corresponding elastic deformations are calculated by BEM and FEM respectively. An iterative staggered algorithm for the electrostatic-elastic coupled field analysis is applied in order to attain the force equilibrium. The natural frequency shifting of the actuator is computed through the linearization of the relation between the electrostatic force and the displacement at the equilibrium. The stiffness matrix of the actuator can be modified into equivalent lumped stiffness at this equilibrium state. The displacement field can be perturbed using a concerned eigenmode profile of the actuator and then the corresponding configuration change of the actuator modifies the electrostatic field and thus the electrostatic force. The equivalent stiffness corresponding to the change of the electrostatic force is then added to lumped elastic stiff-

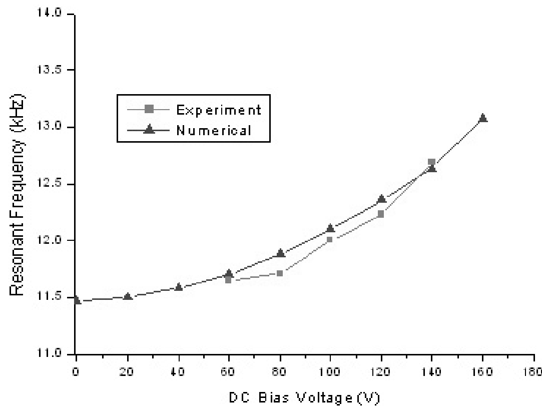


**Figure 18** : Computed and measured natural frequency of the structure for tuning voltages

ness of the system in order to consider the natural frequency shifting. The numerical examples, a simple structure and two actual micro actuator systems, are presented and the computed results are compared with the experimental results of the literatures. From the comparison, the results of the proposed numerical method are very close to the experimental ones.

## References

**Adams, S. G.; Bertsch, F. M.; Shaw, K. A.; Hartwell, P. G.; Macdonald, N. C.; Moon, F. C.** (1995): Capacitance based tunable micro mechanical resonators. *Proc. 8th Inter. Conf. Solid-State Sensors and Actuators (Transducers '95)*, Stockholm, pp. 438-441.

**Francais, O.** (2000): Analysis of a micro actuator with the help of Matlab/simulink: transient and frequency character-istics. *MSM2000*, San Diego, California, USA, pp. 281-284.

**Gaul, L.; Fischer, M.; Nackenhorst, U.** (2003): FE/BE Analysis of Structural Dynamics and Sound Radiation from Rolling Wheels, *CMES: Computer Modeling in Engineering & Sciences*, vol. 3, no. 6, pp. 815-824.

**Han. Z. D.; Atluri, S. N.** (2003): On Simple Formulations of Weakly-Singular Traction & Displacement BIE, and Their Solutions through Petrov-Galerkin Approaches, *CMES: Computer Modeling in Engineering & Sciences*, vol. 4 no. 1, pp. 5-20.

**Katsikadelis, J. T.; Nerantzaki, M. S.** (2000): A boundary-only solution to dynamic analysis of non-homogeneous elastic membranes. *CMES: Computer Modeling in Engineering & Sciences*, Volume 1, Number 3, pp. 1-9

**Lee, K. B.; Cho, Y.-H.** (1998): A triangular electrostatic comb array for micromechanical resonant frequency tuning. *Sensors and Actuators*, A70, pp. 112-117.

**Ljung, P.; Bachtold, M.; Spasojevic, M.** (2000): Analysis of realistic large MEMS devices. *CMES: Computer Modeling in Engineering & Sciences*, 1(1), pp. 21-30

**Meirovitch, L.** (1980): Computational methods in structural dynamics. Sijthoff & Noordhoff.

**Seo, K.-S.; Cho, Y.-H.; Youn, S.-K.** (1998): A tunable optomechanical micromirror switch. *Sensors and Materials*, 10(3), pp. 155-168.

**Shi, F.; Ramesh, P.; Mukherjee, S.** (1996): Dynamic analysis of micro-electro-mechanical systems. *International Journal of Numerical Methods in Engineering*, 39, pp. 4119-4139.

**Tang, W. C.; Nguyen, C. T.-C.; Howe, R. T.** (1989): Laterally driven polysilicon resonant microstructures. *Sensors and Actuators*, A, pp. 25-32.

**Tang, W. C.; Lim, M. G.; Howe, R. T.** (1992): Electrostatic comb drive levitation and control method. *Journal of Microelectromechanical systems*, 1(4), pp. 170-178.

**Ye, W.; Mukherjee, S.** (2000): Design and fabrication of an electrostatic variable gap comb drive in micro-electro-mechanical systems. *CMES: Computer Modeling in Engineering & Sciences*, 1(1), pp. 111-120